



## Upgrade on risk analysis following the 080919 incident in the LHC sector 3-4

*Maciej Chorowski<sup>1</sup>, Jaroslaw Fydrych<sup>1</sup>, Zbigniew Modlinski<sup>1</sup>, Jaroslaw Polinski<sup>1</sup>, Laurent Tavian<sup>2</sup>  
Janusz Wach<sup>1</sup>*

<sup>1</sup> Wroclaw University of Technology, Wroclaw, Poland

<sup>2</sup> CERN, Geneva, Switzerland

---

---

### Summary

**On 19th September 2008, during powering tests of the main dipole circuit in sector 3-4 of the LHC, an electrical fault occurred producing an electrical arc and resulting in mechanical and electrical damage, release of about 6 tons of helium from the magnet cold mass to the insulation vacuum enclosure and consequently to the tunnel, via the spring-loaded relief discs on the vacuum enclosure. The helium discharge from the cold mass to the vacuum enclosure exceeded by an order of magnitude, the maximum credible incident (MCI) flow described in the preliminary risk analysis performed in 1998. Based on the experience gained from the 19<sup>th</sup> September 2008 incident, a new MCI has been formulated and the cryogenic risk analysis has been revised and updated. The recommendations concerning the safety relief system protecting the vacuum vessels and the mechanical properties of the doors installed in the tunnel have been formulated.**

---

### 1. Introduction

The aim of this report is to provide the results of update of the Preliminary Risk Analysis (PRA) of the LHC Cryogenic System. The 19th September 08 incident in the LHC sector due to an electrical arc in the main dipole bus-bar circuit has produced a large helium discharge in the cryo-magnet cryostats, a large helium release in the LHC tunnel as well as blast impact on tunnel ventilation door [1]. The risk analysis of the LHC cryogenic system has to be revised for the redefinition of the cryo-magnet protection against over-pressure and for the personnel underground access.

### 2. Output from the Preliminary Risk Analysis performed in 1999.

The objective of the Preliminary Risk Analysis (PRA) study [2] was to identify all risks to personnel, equipment or environment resulting from cryogenic failures that might accidentally occur within the cryogenic system of Large Hadron Collider in any phase of the machine operation, and that could not be eliminated by design. The recommendations concerning lines of preventive and corrective defence, as well as further, more detailed studies have been then formulated. As the Maximum Credible Incident (MCI) a full break of jumper

connection resulting with about 4250 kg helium relief to the tunnel with a peak flow of about 20 kg/s was identified, although the event was described as physically possible but highly improbable. The second critical event analyzed with respect to the mass of helium discharged to the tunnel was helium flow to the QRL insulation vacuum caused by break of header C and resulting with 3300 kg of helium relieved to the tunnel, albeit with a much lower mass flow, not exceeding 2 kg/s – see Figure 1.

A potential failure caused by the electrical arc in the superconducting cables joint have been identified but underestimated with respect to its consequences and treated as an event covered by the helium flow to the vacuum space. The maximum breach cross-section enabling the helium flow to the vacuum space has been assumed as equal to 5 cm<sup>2</sup>. The resulting diameter of the safety valves protecting the vacuum vessel has been calculated to be of DN90 mm. The valves have been located at each LHC cell with the pitch of 107 m.

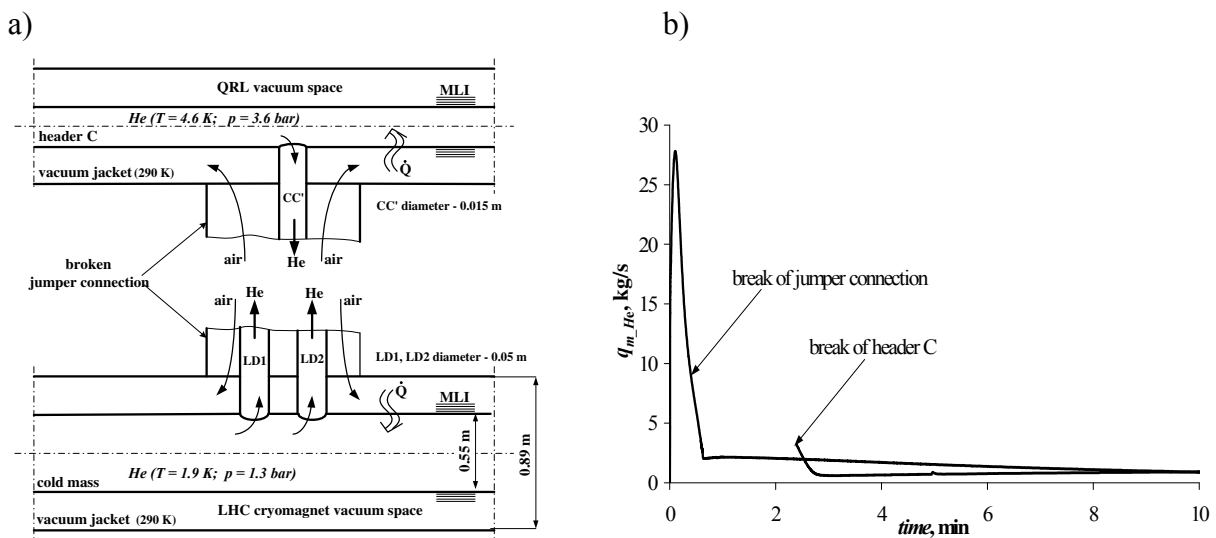


Figure 1. Preliminary Risk Analysis worst case scenario, a) – schematic depiction of full break of jumper connection, b) – helium flows to the LHC tunnel

### 3. Redefinition of Maximum Credible Incident with respect to helium flow to cryostat insulation vacuum – full cut of interconnecting pipes

In the Preliminary Risk Analysis [2] it has been assumed that the helium flow to the vacuum space will be limited by a process pipe or cold mass enclosure breach not exceeding a cross-section of 5 cm<sup>2</sup>. To avoid the over-pressurization of the vacuum space, two safety valves of the diameter DN90 have been installed in-between vacuum barriers located at the distance of 214 m. During the 19th September 2008 incident the helium was discharged to the vacuum space through the total cross section of about 166 cm<sup>2</sup>, the value exceeding the PRA assumption of 5 cm<sup>2</sup> by more than the order of magnitude (compare Table 1). The underestimated available safety valves cross-section of 127 cm<sup>2</sup>, has caused pressurization of the vacuum space to about 8 bar, resulting in severe direct and collateral damages. To avoid potential similar damages resulting from faulty electrical joint creating the electrical arc in the future, the Maximum Credible Incident (MCI) has to be redefined. A new MCI assumes a full cut of the interconnecting pipes in-between two magnet cold masses. The comparison of the cross-sections available for helium flow to the vacuum space assumed in PRA, observed on the 19th September 2008, and resulting from the assumption of full cut of all the interconnection pipes (redefined MCI) is given in Table 1. However in case of full cut of the

interconnecting pipes, a limiting factor which has to be taken into account is the available free cross-section for longitudinal flow in the magnet cold-mass lamination, limited to about  $60 \text{ cm}^2$ . Therefore, even in the case when breaches appearing in the interconnection are larger than  $2 \times 60 \text{ cm}^2$ , the magnet laminations will limit the total effective opening to  $120 \text{ cm}^2$ .

**Table 1.**

Available cross-section for different failure scenarios [ $\text{cm}^2$ ]

Interconnection pipe	Preliminary Risk Analysis [2]	19th Sept. 08 Incident	Maximum Credible Incident
Bus-bar piping	5	2 x 32	6 x 32
Line E	0	2 x 50	2 x 50
Line C via Line C'	0	1.8	2 x 1.8

Figure 2 shows the location of the interconnecting pipes damages during the 19th September 2008 incident, including two beam tube cuts. A new MCI takes into account the cut of the upper bus-bar piping, not opened during the 19th September 2008 incident.

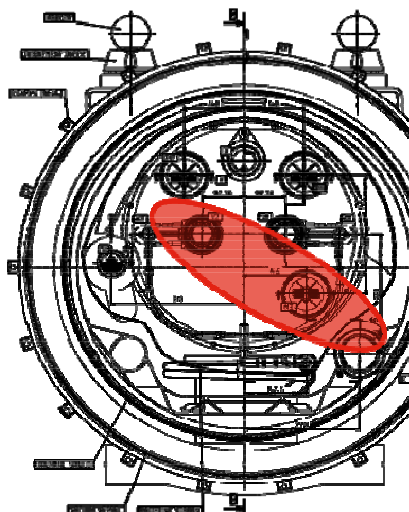


Figure 2. Direct internal pipe damages during the 19th September 2008 incident

#### 4. Development of mathematical model

Mitigation of the damages resulting from the helium inflow to the vacuum space needs good understanding of the helium parameters evolution resulting from energy and mass transfer processes depicted schematically in Figure 3.

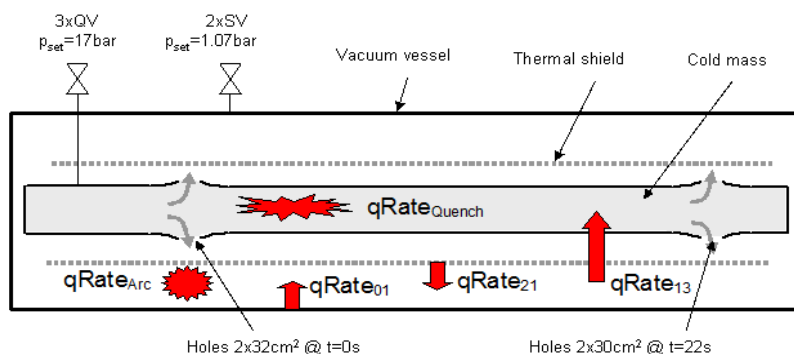


Figure 3. Scheme of the mathematical model describing the helium parameters evolution

A mathematical model enabling the calculation of the helium thermodynamic parameters in the cold mass and vacuum space, as well as corresponding helium flows, has been developed. The model enables the helium parameters simulation from first principles, using a lumped parameter approach helium parameters in the cold mass and vacuum space enclosures; and one-dimensional approach – to calculate longitudinal helium flows. The model input data are the following heat flows:

- $q_{RateQuench}$  – heat transfer from the quenched magnets to the cold mass helium,
- $q_{RateArc}$  – heat transfer from electrical arc to the helium in the vacuum space,
- $q_{Rate01}$  – heat transfer from the vacuum vessel to the helium in the vacuum space,
- $q_{Rate21}$  – heat transfer from the aluminum shield to the helium in the vacuum space,
- $q_{Rate13}$  – heat transfer from the helium in the vacuum space to the cold mass helium.

#### 4.1. Heat transfer from the quenched magnets to the cold mass helium – $q_{RateQuench}$

The heat flux resulting from the magnet quench has been scaled with the current from the experimental curve shown in Figure 4 [5]. The data shown in Figure 4 have been registered for a 13 kA quench of the String 1 magnets (three dipoles and one quadrupole). At the beginning the heat dissipated at the cold mass helium was of the order one MW, to fall almost linearly with a change in a slope after about 10 s. The scaling with the current has been done according to the equation (1), taking into account a number of the quenched magnets.

$$E_{mag} = \frac{1}{2} L \cdot I^2 \quad (1)$$

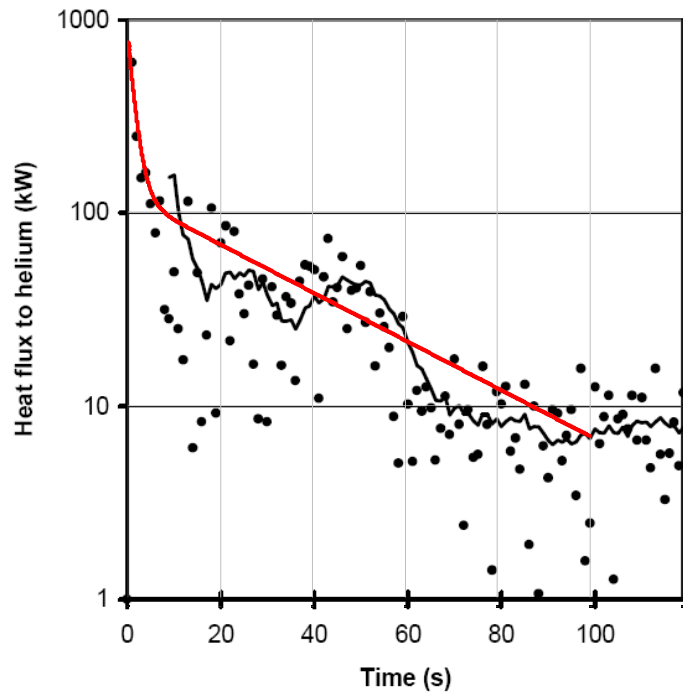


Figure 4. Heat flux transferred to cold mass helium after main dipole quench [5]

#### 4.2. Heat transfer from electrical arc to the helium in the vacuum space – $q_{RateArc}$

Figure 5 shows the arc power resulting from the electrical arc during the 19th September 2008 incident for an initial arc current of 8.7 kA. In the mathematical model, the electrical arc heat flux has been conservatively scaled with the second power of the initial current according to the equation (2).

$$Q_{ele\_arc}(I_{arc}) = \left( \frac{I_{arc}}{8.7kA} \right)^2 Q_{ele\_arc}(8.7kA) \quad (2)$$

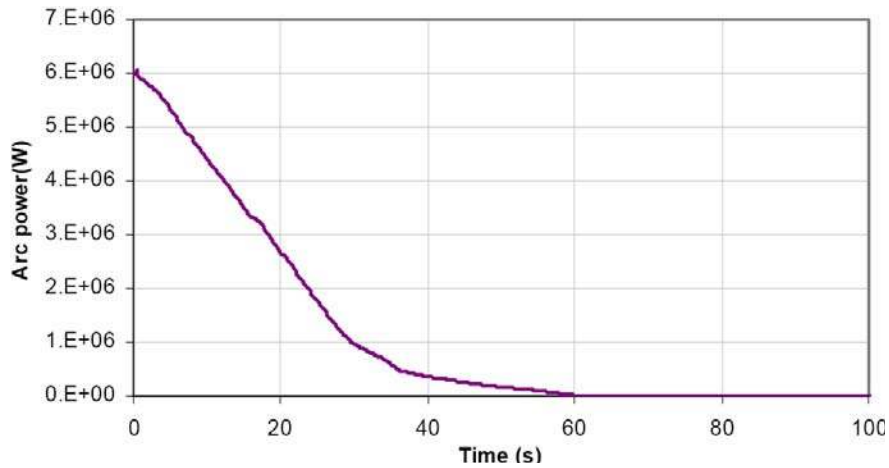


Figure 5. Heat flux resulting from electrical arc during the 19th September 2008

#### 4.3. Convective heat transfer flows – $q_{Rate01}$ , $q_{Rate21}$ and $q_{Rate13}$

The scheme of convective heat transfer processes following the breach in interconnecting pipe or cold mass shrinking cylinder is depicted in Figure 6. This way of heat transfer is observed from the vacuum vessel to the helium in the vacuum space ( $q_{Rate01}$ ), from the aluminium shield to the helium in the vacuum space ( $q_{Rate21}$ ) and from the helium in the vacuum space to the cold mass helium ( $q_{Rate13}$ ). The heat fluxes denoted as  $q_{Rate01}$ ,  $q_{Rate21}$ ,  $q_{Rate03}$  are the fluxes transferred between the helium in the vacuum space and vacuum vessel, aluminium shield, cold mass.

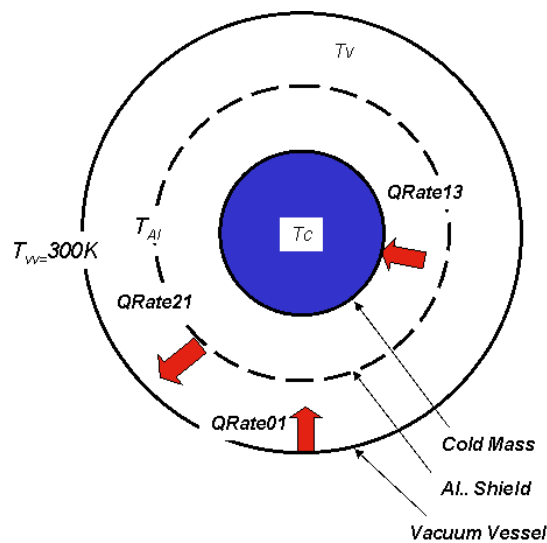


Figure 6. Scheme of the gas heat transfer in the vacuum space.

For the purpose of this analysis the heat transfer between the helium filling the cold mass or vacuum space and the magnet construction element (vacuum vessel, aluminium shield, shrinking cylinder) have been assumed to be governed by natural convection mechanism. In reality, due to the longitudinal helium flow, the process must lay somewhere between the natural and forced convection, hence the heat transfer coefficient has been increased to fit the experimental data. The governing equations describing the processes are given in Table 2 in which:

- $T_c, T_v$  are the helium temperatures in cold-mass and vacuum enclosures,
- $T_{Al}, T_{vv}$  are the temperatures aluminium shield and vacuum vessel,
- $A_c, A_{Al}, A_{vv}$  are the heat exchange areas of cold-mass, aluminium shield and vacuum vessel.

**Table 2.**

Natural convection heat transfer processes following the helium flow to vacuum space

Nr.	Process	Equation
1	Heat transfer from vacuum vessel to helium in vacuum space – $Q_{Rate01}$	$Q_{Rate01} = A_{vv} \cdot h_{01} \cdot (T_{vv} - T_v)$
2	Heat transfer from aluminum shield to helium in vacuum space – $Q_{Rate21}$	$Q_{Rate21} = 2 \cdot A_{Al} \cdot h_{01} \cdot (T_{Al} - T_v)$
3	Heat transfer from vacuum helium to cold mass helium – $Q_{Rate13}$	$Q_{Rate13} = A_{Al} \cdot h_{13} \cdot (T_v - T_c)$

As mentioned above, it has been assumed that the heat transfer processes listed in Table 2 can be described as natural convection and the natural convection heat transfer coefficients in an annular circular enclosure can be derived from the equation (3):

$$h_c = \frac{Nu \cdot k_{He}}{L} \text{ where characteristic length } L = D_2 - D_1 \quad (3)$$

The heat transfer conditions with respect to the combination of Grashoff and Prandtl  $GrPr$  numbers, in geometry depicted in Figure 7, are specified in Table 3.

**Table 3.**

Natural convection heat transfer coefficients

Heat transfer condition	$GrPr$	$Nu$	$Gr$
Suppressed motion	$GrPr < 10^3$	$Nu = \frac{D_2/D_1 - 1}{\ln(D_2/D_1)} = B$	$Gr = \frac{g\beta\rho^2(T_2 - T_1)L^3}{\mu^2}$
Cellular motion	$10^3 < GrPr < 10^6$	$Nu = 0.11 \cdot B \cdot (Gr \cdot Pr)^{0.29}$	$Gr = \frac{g\beta\rho^2(T_2 - T_1)L^3}{\mu^2}$
Turbulent flow	$10^6 < GrPr < 10^8$	$Nu = 0.4 \cdot B \cdot (Gr \cdot Pr)^{0.2}$	$Gr = \frac{g\beta\rho^2(T_2 - T_1)L^3}{\mu^2}$

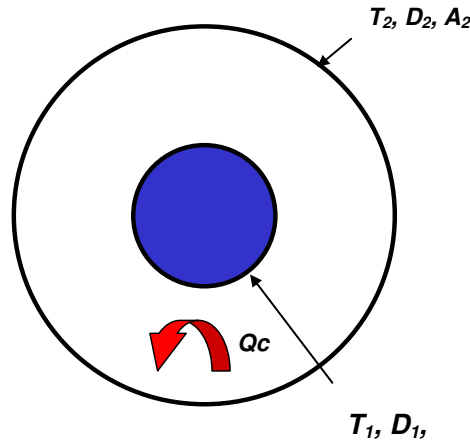


Figure 7. Schematic depiction of natural convection in a circular channel.

#### 4.3.1. Model tuning

The model tuning has been performed on the basis of the cold mass helium pressure evolution measured during the 19th September 2008 incident. The parameter that has been adjusted to obtain the calculated peak pressure equal to the measured maximum helium pressure in the cold mass [1] was the heat transfer coefficient calculated from the formula (3) for the conditions specified in Table 3. A perfect match of the registered and calculated peak pressure value have been obtained for the heat transfer multiplication coefficient of 1.6. The heat transfer coefficient adjusted value exceeds the free convection value and proves that the conditions of heat transfer process are in-between natural and forced convection.

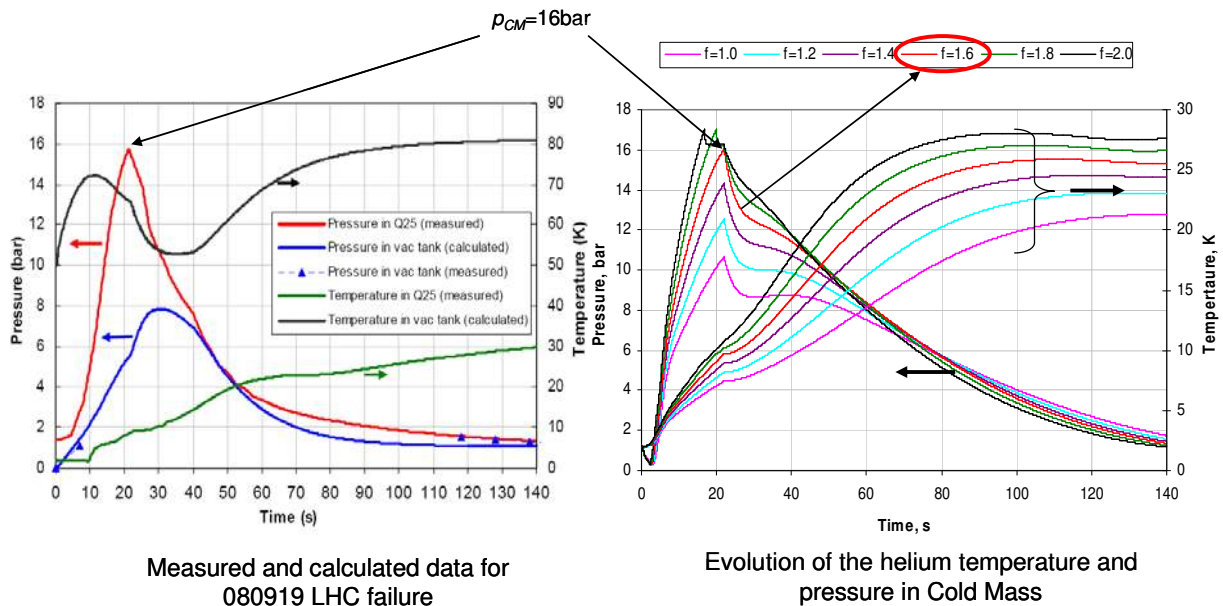


Figure 8. Model tuning by adjusting a free convection heat transfer coefficient.

### 5. Modeling of the 19th September 08 incident

The model has been validated by the reproduction of the helium parameters following the 19th September 2008 incident. Then the sequence of events given in Table 4 was taken as a set of initial conditions for the modelling.

**Table 4.**

Sequence of events during the 19th September 2008 incident

No.	Time , s	Event	Remark
1	0	M3 pipe break, origin of two holes of the area $2 \times 32 \text{ cm}^2$	The event caused by the electric arc at the current $I=8.7 \text{ kA}$
2	5	Quench of a half-cell (4 magnets) at the current $I=8.7 \text{ kA}$	The event triggered by fast current discharge ramp and electrical noise
3	22	Pipe break at the adjacent inter-connection, origin of two $32 \text{ cm}^2$ holes – collateral damage	The event caused by the pressure rise in the vacuum space

The comparison of modelling results with the directly (cold mass pressure, cold mass temperature) and indirectly (vacuum space pressure, vacuum space temperature) measured helium parameters evolution is given in Figure 9. The calculated pressure profile is in good accordance with the measured curve and some minor differences can be explained as follows. The change of slope of the measured pressure curve visible in the time instant of 40 s can be caused by further collateral damages and new breaches in the vacuum bellows of the interconnection region which were not taken into account in the model calculations. A visible cold mass pressure drop in-between the origin of the breach of the interconnecting pipes in the calculated curve and not confirmed by the measurements (a slow pressure increase from the beginning, change of slope after the half-cell quench), can be explained by the assumption of instantaneous cut of the interconnecting pipes and the supposition that the arc heat is transferred to the vacuum space helium only. The measured delay in the increase of the cold mass temperature is most probably caused by the adiabatic compression of the helium following directly the magnet resistive transitions energy dissipation, according to two-volume model described in [5]. The modelled maximal vacuum space helium pressure exceeds 8 bars and corresponds to the pressure estimated from the observation of mechanical damage of the vacuum barrier bellow. The modelled evolution of helium temperature in the vacuum space (Figure 9, right) differs significantly from the data shown in Figure 9 (left), but the parameter has not been measured and mere calculated with a simplified approach [1].

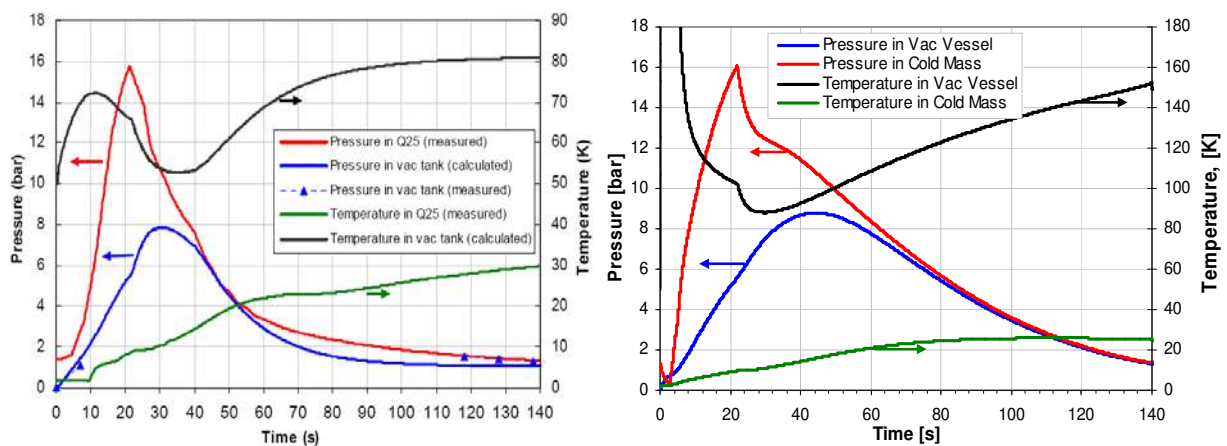


Figure 9. Measurements (left) and modeling (right) of the 19th September 2008 incident.

The modelled helium flows during the 19th September 2008 incident are shown in Figure 10. The quench valves did not open, a peak helium mass flow from the cold mass to the vacuum space was about  $30 \text{ kg/s}$ , while the helium outflow to the tunnel reached about



11 kg/s. Figure 11 gives the time evolution of the heat fluxes – model input, while Figure 12 shows the corresponding heat transfer coefficients for the heat fluxes listed in Table 2. The values of the heat transfer coefficients lay in the range typical for convective heat transfer.

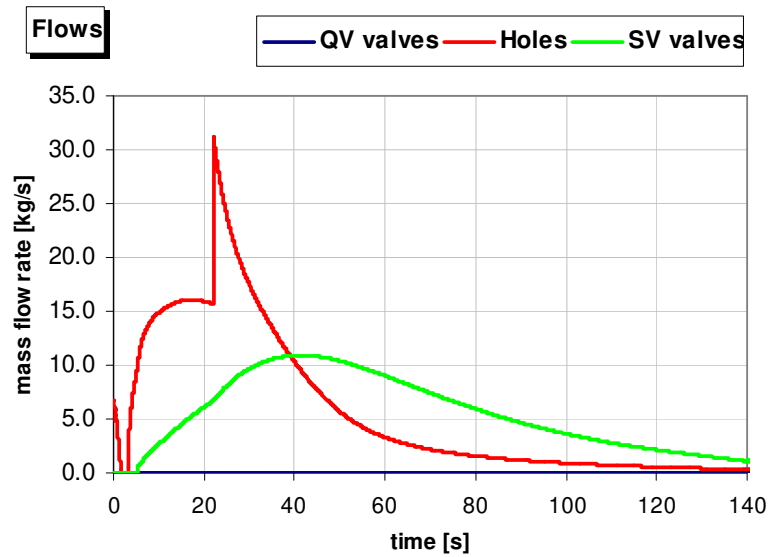


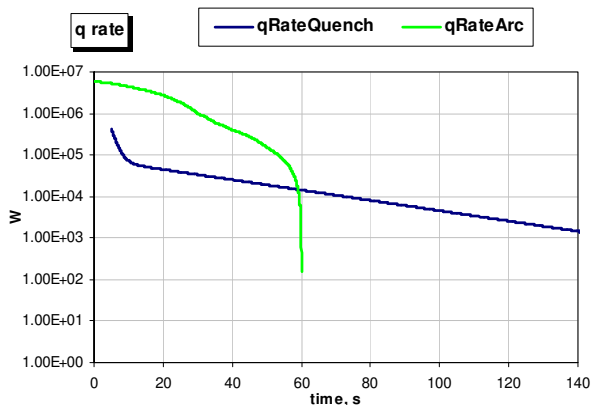
Figure 10. Modeling of the 19th September 2008 incident – helium mass flows through the holes and SV (vacuum vessel safety valves)

The flow decrease through the breaches and its rapid increase after 5 s as seen in Figure 10 is caused by low heat transfer intensity during the first 5 s and later heat impact to the cold mass helium resulting from the quench of the magnets (see Figure 11).

Figure 12 shows the evolution of the calculated heat transfer coefficients:

- $h_{01}$ : to the helium in the vacuum space from the vacuum vessel,
- $h_{21}$ : to the helium in the vacuum space from the aluminium shield,
- $h_{13}$ : to the cold mass helium from the helium in the vacuum space.

a)



b)

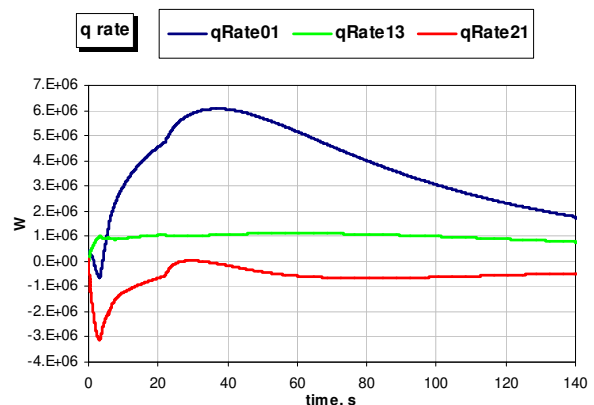


Figure 11. Modeling of heat fluxes – model input for the 19th Sept. 2008 incident.

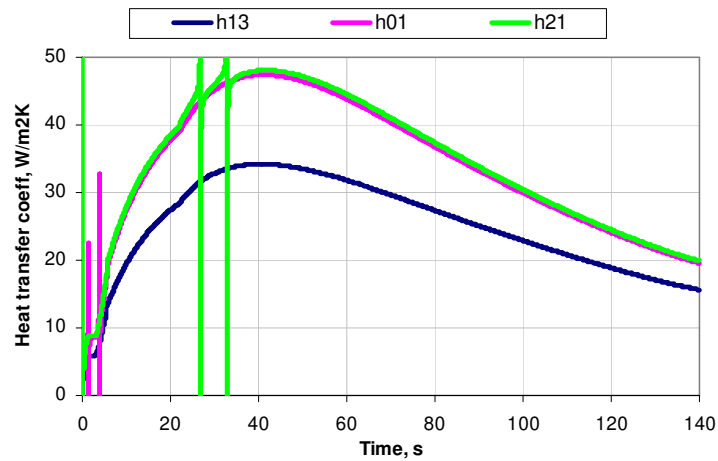


Figure 12. Evolution of heat transfer coefficients

## 6. Modelling of the MCI (Maximum Credible Incident)

The consequences of the redefined Maximum Credible Incident (see Table 1) have been modelled, enabling a proper scaling and configuration of the vacuum vessel safety valves. The mechanical destruction of the interconnecting pipes according to the MCI has been accompanied by simultaneous occurring of the following events:

- full break of the pipes resulting with the total area of the holes:  $6 \times 32 \text{ cm}^2 = 192 \text{ cm}^2$ ,
- simultaneous quench of two cells (16 magnets) at the current of 13.1 kA.

In spite of the total area of the breaches equal to  $192 \text{ cm}^2$ , the flow is restricted by the longitudinal cold mass free flow area of  $120 \text{ cm}^2$ ; hence the simulations have been performed for this value ( $120 \text{ cm}^2$ ).

The simulations have been performed for three Safety Valves configurations: original (prior to 19<sup>th</sup> September 2008 incident), temporary (acceptable for low energy runs) and final (recommended) - see Figures 13 to 15.

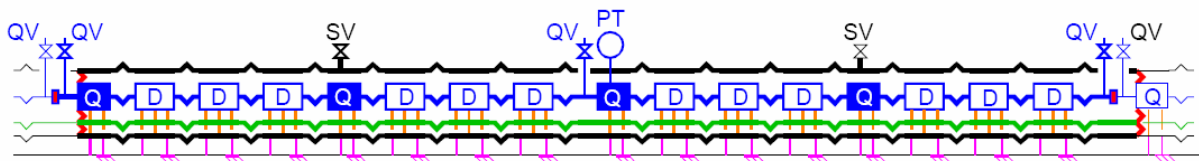


Figure 13. Original (prior to 19th September 08 incident) SV scheme.

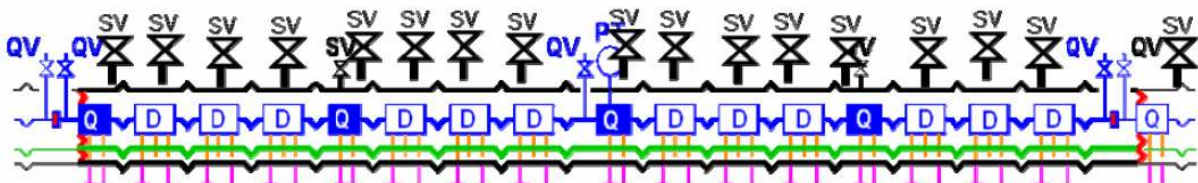


Figure 14. Final (recommended) SV scheme.

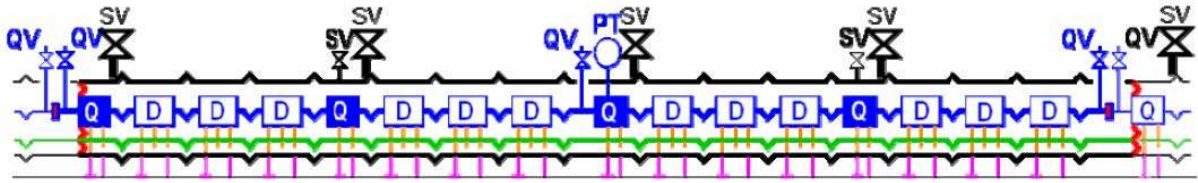


Figure 15. Temporary (acceptable for low energy runs) SV scheme

### 6.1. MCI with original SV scheme

Figures 16 and 17 present the modeling results of the Maximum Credible Incident (MCI) with original SV scheme. The maximum pressure in vacuum space reaches the value of 12 bar and exceeds the pressure estimated for 19th September 2008 incident by 4 bar. The pressure increase in cold mass helium is mitigated by the helium outflow to the vacuum space, while the quench valves (QV) remain closed.

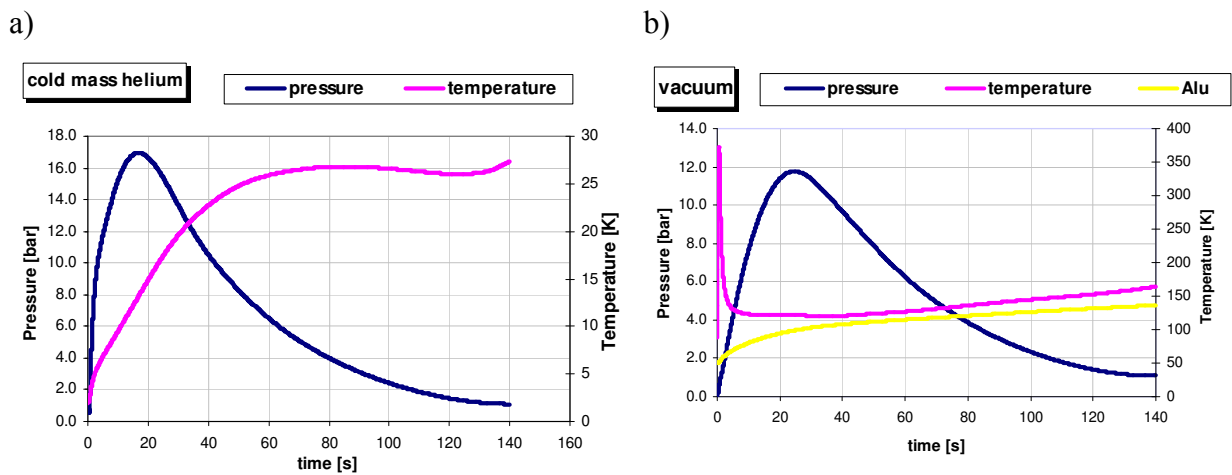


Figure 16. Modelling results with original SV configuration scheme.

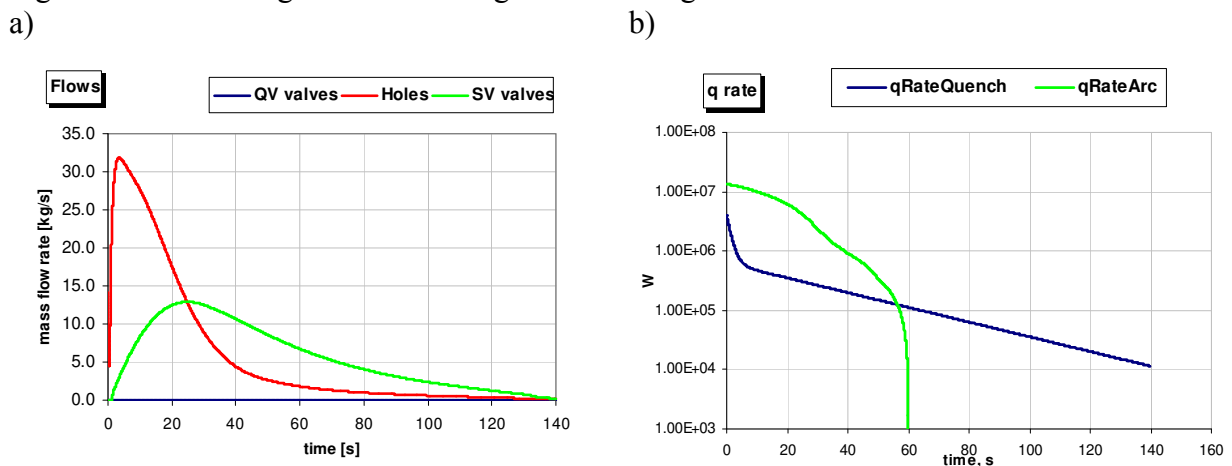


Figure 17. Modeling results with original SV configuration scheme, a) – helium flow through the holes, QV valves and SV valves, b) – heat fluxes to the helium.

### 6.2. MCI with temporary SV scheme

Figure 18 and 19 present the modeling results of the MCI with temporary SV scheme. The temporary SV scheme has been implemented in the sectors remained cold after the 19th September 2008 incident. This scheme uses all the ports on the vacuum vessel which are available to install additional safety valves (see Figure 15). In addition to the 2 existing SV of DN90, 13 SV of DN100 are available given a total cross section of 1270 cm<sup>2</sup> enable to

discharge helium flow from the vacuum space. The temporary scheme is acceptable for low-energy runs, when the stored energy is much below the nominal.

In case of MCI, the vacuum space helium pressure will reach the value of about 2.4 bar, still exceeding the design pressure by 1.1 bar. Taking into account the operation planning of the LHC, full energy runs is not foreseen with the temporary SV scheme. Nevertheless, it is recommended to reinforce the machine fixed-point anchoring for taking this additional pressure force.

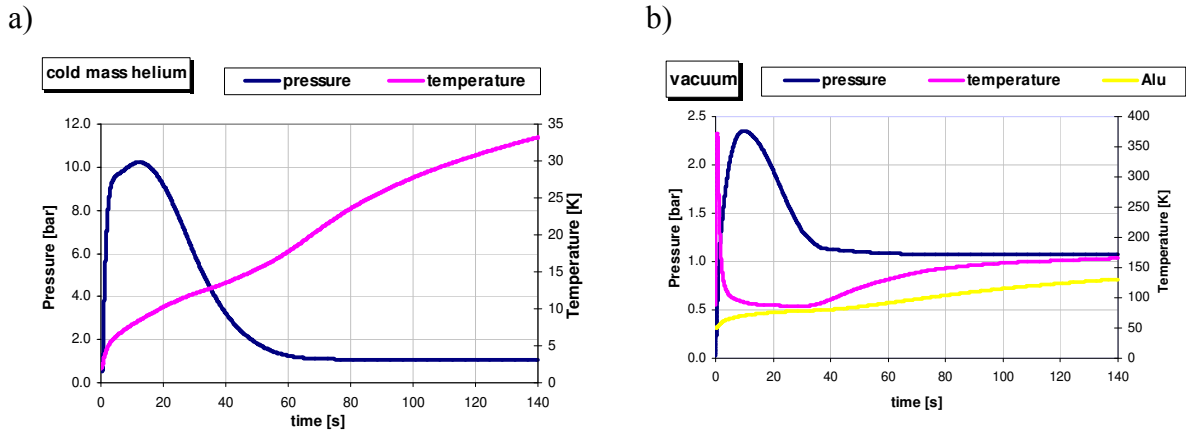


Figure 18. Modeling results with temporary SV configuration scheme, a) – cold mass helium parameters, b) – vacuum space helium parameters and temperature of the aluminium thermal screen

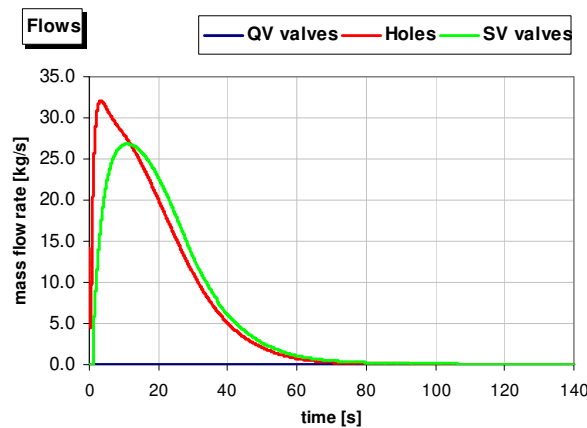


Figure 19. Helium flow through the holes, QV valves and SV valves following the MCI with temporary SV scheme

### 6.3. MCI with final SV scheme

The MCI modelling results for final vacuum vessel safety valves configuration are shown in Figures 20 and 21. The additional valves are the SV valves of DN200 installed at each dipole position and guaranteeing the helium flow cross section of 4190 cm<sup>2</sup>. The helium pressure in the vacuum space would not exceed 1.2 bar and the helium flows through the holes (interconnecting pipes breaches) and vacuum space safety valves are close to each other. The cold mass helium pressure oscillations during the first 20 s are caused by the changes of the heat transfer intensity to the cold mass helium from the helium filling the vacuum space.

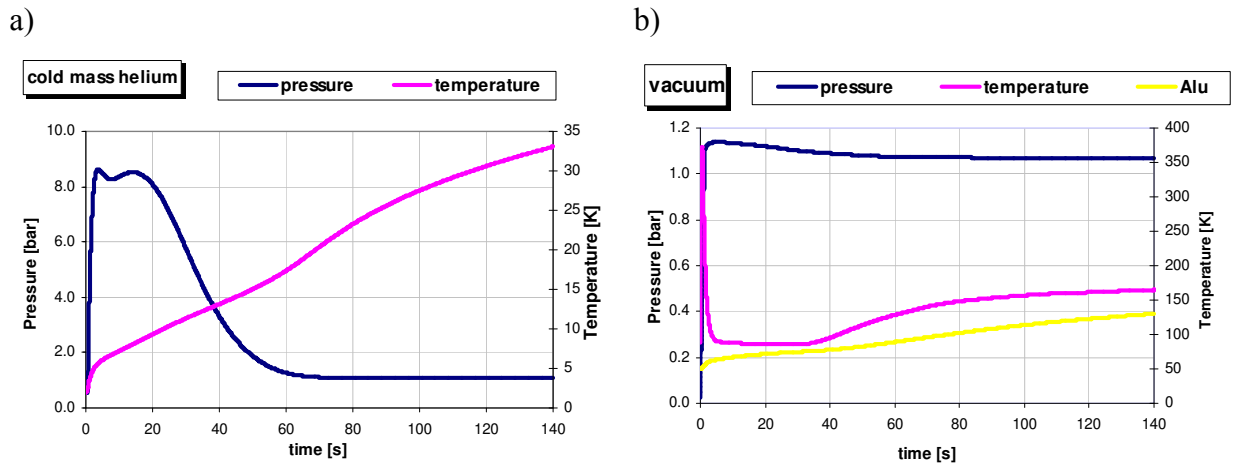


Figure 20. MCI modeling results with final SV configuration scheme, a) – cold mass helium parameters, b) – vacuum space helium parameters and temperature of the aluminium thermal screen

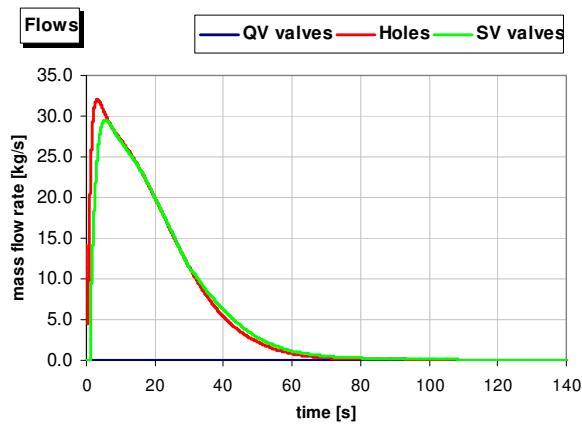


Figure 21. Helium flow through the holes, QV valves and SV valves following the MCI with final SV scheme

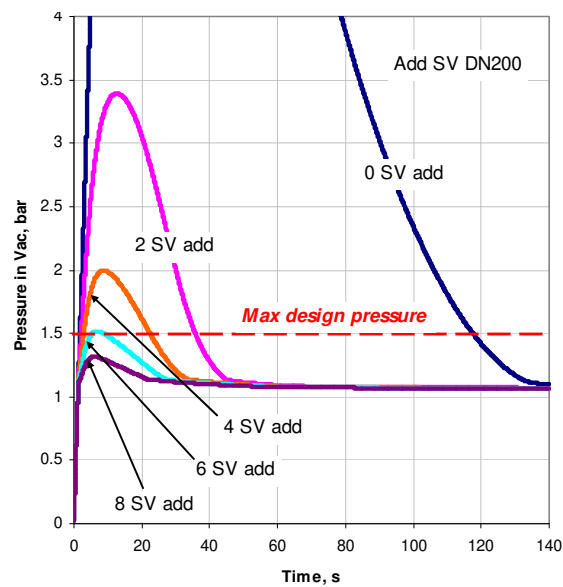


Figure 22. Parametric analysis - Helium pressure evolution in vacuum vessel for different number of additional DN200 SV per sub-sector

Figure 22 shows a parametric analysis given the vacuum-enclosure pressure evolution for different number of DN200 safety valves added to protect a sub-sector. To avoid over pressurization of the vacuum space at least 8 DN200 valves should be added in-between the vacuum barriers delimiting a sub-sector. Final configuration assumes 12 additional valves and provides reasonable redundancy and safety margin.

## **7. Analysis of the pressure rise in the LHC tunnel following the helium significant discharge**

During the CERN incident on 19th September 2008 the amount of about 6 ton of helium has been released into the LHC tunnel with consequence of pressure rise in the wake of which ventilation doors have been blown up. The present analysis of the pressure rise in the LHC tunnel is inspired by safety reasons. Its goal is to identify pressure rise mechanism, estimate maximum pressure rise and assess whether or not additional phenomena like shock wave could have taken place.

### **7.1. The pressure rise mechanism**

Due to electrical arc the cold mass helium enclosure has been destroyed, leading to release of helium into the insulation vacuum of the cold mass. In consequence the relief discs on the vacuum enclosure opened when the pressure exceeded atmospheric and relieved the helium to the tunnel which sees its pressure increasing. The pressure rise mechanism in the tunnel can be described as follows.

The helium of low temperature (about 160 K after 140 s – compare Figure 9) after leaving the vacuum enclosure suddenly came into contact with “hot” tunnel walls, which temperature can be assumed to be of about 300 K. In the wake of it helium masses rapidly expanded. Consequently, its volume dramatically increased by the factor up to 2 orders of magnitude. The phenomenon can be expressed in terms of volume production and helium leakage can be considered as a volume source. When some amount of volume is released into confined space it causes a pressure rise. This can be dangerous if confinement walls can't withstand the developed pressure. Such phenomenon is known as “physical explosion”. During physical explosion no exothermic reaction takes place and pressure rise is basically a consequence of phase transition or cold gas expansion.

When enclosure is partially confined, the pressure development in time is a result of difference between the volume production rate and expansion rate due to volume escape via the openings. The final overpressure is thus result of its dynamics and duration time of the phenomenon. In physical explosion the pressure wave travels at the speed of sound, but because of lack of exothermic reaction, detonation phenomenon is excluded. This in consequence excludes pressure rise above maximum pressure of explosion i.e. pressure resulting from compression of produced volume to volume of confinement.

The case of CERN 19th September 2008 incident can be classified as a physical explosion. The volume production was driven by the heat delivered from tunnel walls, which can be considered as infinite heat source. Such assumption can be justified because the tunnel is underground structure and the rock mass surrounding the tunnel can maintain steady temperature of the walls. Besides, such assumption corresponds to the worst case condition, which means that the estimated pressures will be of the highest possible value to obtain and the real pressures can be only lower.

According to [1] the helium leakage was a two stage process. In the first stage about 2 t of helium, were rapidly released to the tunnel. The mass flow rate particularly for the first 800 – 1000 kg, was estimated to be 20 kg helium per second. In the second stage another 4 t of helium were lost, but at much lower flow rates. The total loss of inventory thus amounts to

about 6 t, out of 15 t initially in the sector. Taking the data into account it is justified to conclude that the first stage of the leakage was critical for pressure development.

The helium was released to the LHC tunnel sector of volume  $V_o = 33000 \text{ m}^3$  and length  $L = 3.3 \text{ km}$ . The following Table 5 presents volume of different helium masses at different temperatures and the helium mass ratio to the sector volume.

**Table 5.**

Helium volume  $V_{He}$  and its ratio to tunnel sector volume  $V_o$  for different temperatures and helium masses at the atmospheric pressure

Mass of helium [kg]	100 K		200 K		300 K	
	$V_{He} [\text{m}^3]$	$V_{He}/V_o$	$V_{He} [\text{m}^3]$	$V_{He}/V_o$	$V_{He} [\text{m}^3]$	$V_{He}/V_o$
800	1663	0.05	3326	0.10	4990	0.15
1000	2079	0.06	4158	0.13	6237	0.19
2000	4158	0.13	8316	0.25	12474	0.38
6000	12474	0.38	24948	0.76	37422	1.13

It can be seen that during the first stage of the leakage, the helium volume at atmospheric pressure makes from 19 to 38 percent of total tunnel volume. It means that the leakage process can be considered as a volume expansion to partially confined space.

## 7.2. Static approach

The first approach to assessment of the maximum pressure resulting from helium release can be calculated from static consideration by neglecting the dynamics of the process. The calculations have been performed under the following assumptions.

- There is clear interface between air and helium (the gases do not mix together).
- The tunnel is tight so there is no escape of air or helium from it.
- During helium injection air remaining in the tunnel is compressed. This process can be considered adiabatic or isothermal depending on how fast or slow is the compression.
- During whole process the pressure  $p$  in is uniform along the tunnel.
- The initial temperature of air in the tunnel is  $T_o = 300 \text{ K}$ , and the initial pressure is atmospheric i.e.  $p_o = 1 \cdot 10^5 \text{ Pa}$ .
- The temperature of injected helium remains constant and is equal  $T$ .

Figure 23 shows a sketch explaining helium injecting to the tunnel sector where:

- $L$ : tunnel length,
- $A_o$ : tunnel cross-section area,
- $V_{He}$ : volume occupied by helium,
- $V_A$ : volume occupied by air after injection.
- (I): tunnel of volume  $V_o$  filled only with air of pressure  $p_o$ .
- (II): tunnel after injecting some amount of helium under assumption that both gases do not mix together.

Again it is worth to mention that the above assumption corresponds to worst case giving maximum attainable pressure.

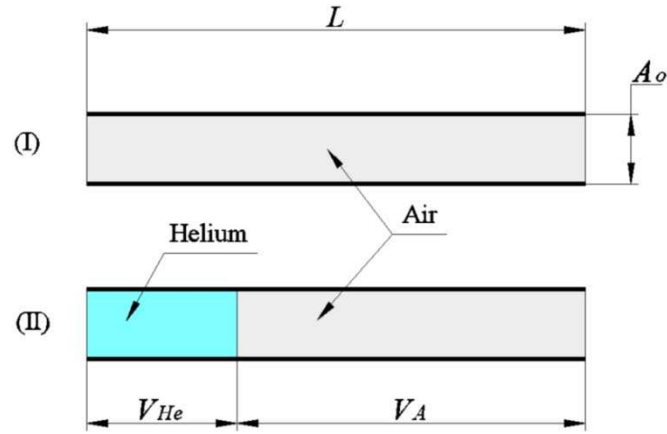


Figure 23. Sketch explaining helium injecting to the tunnel sector.

The governing equations in the case of adiabatic air compression are:

$$\begin{cases} V_A + V_{He} = V_o \\ pV_{He} = mR_{He}T \\ p_o V_o^{\gamma_{Air}} = pV_A^{\gamma_{Air}} \end{cases}, \quad (4)$$

where:

- $V_{He}$ : volume occupied by helium,
- $V_A$ : volume occupied by air after injection,
- $m$ : mass of the injected helium,
- $R_{He}$ : helium specific gas constant
- $\gamma_{Air}$ : specific heat ratio of air.

In the case of isothermal air compression in the last equation of system (4) the variable  $\gamma_{Air}$  should be replaced by one. In this case the pressure  $p$  can be easily calculated from following expression:

$$p = \frac{V_o p_o - mR_{He}T}{V_o}. \quad (5)$$

The resulting pressures obtained from solving the system (4) and equation (5) for  $V_o = 33000 \text{ m}^3$  (effective cross-section  $10 \text{ m}^2$  and length  $33000 \text{ m}$ ) are summarized in Table 6.

**Table 6.**

Maximum pressure attained after injecting of different mass of helium at different temperatures.  $p_{ad}$  – pressure attained during adiabatic air compression and  $p_T$  – during isothermal.

Mass of helium [kg]	Pressure [MPa]					
	100 K		200 K		300 K	
	$p_{ad}$	$p_T$	$p_{ad}$	$p_T$	$p_{ad}$	$p_T$
800	0.109	0.107	0.118	0.113	0.127	0.120
1000	0.112	0.108	0.123	0.117	0.134	0.125
2000	0.123	0.117	0.144	0.133	<b>0.165</b>	0.150
6000	0.165	0.150	0.226	0.200	<b>0.284</b>	0.250



The maximum pressure which can be attained after injecting helium into tunnel sector is 0.284 MPa, which can happen when whole helium mass (6 t), which was lost during incident will be injected into tunnel at temperature 300 K causing adiabatic air compression. For the first – the fastest – stage (2 t leakage) the pressure rise should be about 0.165 MPa. For isothermal air compression the corresponding values are lower. Taking into account that 30% of helium was released fast and 60% slow, one can assume that the first stage of air compression should be adiabatic while second isothermal. To verify this assumption air temperature rise  $\Delta T$  during adiabatic compression has been calculated and resulting increase of its internal energy  $\Delta U$ . The latter corresponds to amount of heat  $Q$  that has to be transferred to the wall in order to maintain isothermal condition of air compression. Results are given in Table 7.

**Table 7.**

Air temperature rise during adiabatic compression and amount of heat  $Q$  that must have been carried away from air to provide for its isothermal compression.

Mass of helium [kg]	Necessary heat transfer $Q$ and air temperature rise $\Delta T$					
	100 K		200 K		300 K	
	$Q$ [GJ]	$\Delta T$ [K]	$Q$ [GJ]	$\Delta T$ [K]	$Q$ [GJ]	$\Delta T$ [K]
2000	0.523	18	0.963	33	1.346	46
6000	1.346	46	2.286	79	3.034	104

To use above results it is necessary to compute heat transfer time-constant  $\tau$ . This can be calculated from the following equation:

$$\tau = \frac{c_{Air} m_{Air}}{kF} \quad (6)$$

where:

- $c_{Air}$ : specific air heat (1000 J/kg),
- $m_{Air}$ : mass of air occupying the tunnel sector (29 t),
- $k$ : overall heat transfer coefficient ( $0.5 \text{ Wm}^{-2}\text{K}^{-1}$ ),
- $F$ : tunnel wall surface ( $3.984 \cdot 10^4 \text{ m}^2$ ).

For the corresponding values, the calculated time-constant is 25 min, what means that heat transfer process to complete needs more than  $4\tau = 100$  min.

Taking into account the time scale and amount of heat, it is very unlikely that the air compression would be isothermal. Therefore, allowing for slight heat transfer, one should assume polytropic air compression with polytropic exponent close to isentropic one, rather than to one which stands for isothermal process.

Thus the pressure range in the tunnel can be estimated to be of about 0.135 MPa assuming the relieved helium temperature to be of about 160 K and adiabatic compression of the air in the tunnel. Of course allowing for some air escape through shafts and other possible openings the real pressure range can be somewhat slightly smaller.

### 7.3. Analysis of the process dynamics

The real expansion of helium into the tunnel is a dynamic process. During the process the pressure increase is caused by volume production due to the helium leakage. Resulting pressure rise depends on helium mass flow rate. The fastest the flow the highest pressure rise rate. On the other hand taking into account that the fastest stage can be considered as a volume expansion to partially confined space there is helium expansion which acts in opposite

direction and brings about decreasing the rate of pressure rise. Thus there is a sort of competition between volume production and volume expansion. If rate of both are equal then no pressure rise should be observed. If production rate exceeds expansion rate the pressure should increase while the opposite relation does the reverse.

It has been estimated that the highest mass flow rate of helium (in first stage) is 20 kg/s. Taking this into account, the tunnel cross-section area  $A_o = 9.9 \text{ m}^2$ , and the helium density  $\rho_{He} = 0.16 \text{ kg/m}^3$  (at 300 K and 0.1 MPa) the flow velocity can be calculated from equation of continuity to be about 12.6 m/s. It is much less than sound velocity in air (330 m/s) and sound velocity in helium (1018 m/s). This means that presumption of uniform pressure rise along the tunnel can be justified. This has been verified numerically by modeling volume injection into tunnel by adapting numerical model from [6]. The one dimension model of air flow has been assumed and governing equations are equation of continuity

$$\frac{\partial \rho}{\partial t} = -\rho \frac{\partial v}{\partial x} - v \frac{\partial \rho}{\partial x} + W, \quad (7)$$

where term  $W$  is internal mass rate production density and represents source of helium mass injection and the momentum equation (Navier–Stokes or Euler after omitting the last term of right hand side in equation (8))

$$\rho \frac{\partial v}{\partial t} = -\rho v \frac{\partial v}{\partial x} - \frac{\partial p}{\partial x} + \frac{4}{3} \eta \frac{\partial^2 v}{\partial x^2}. \quad (8)$$

Where:

- $\eta$ : dynamic viscosity (assumed for air to be  $1.5 \cdot 10^{-4} \text{ Ns/m}^2$ ),
- $v$ : fluid velocity
- $p$ : pressure along tunnel.

The last equation (9) is equation of adiabatic process

$$p \rho^{-\gamma} = \text{const} \quad (9)$$

The tunnel is assumed to be a horizontal tube of length  $L = 3300 \text{ m}$  and the cross-section area  $A_o = 9.9 \text{ m}^2$ . The left end of the tube has spatial coordinate  $x = 0$  and the right  $x = L$ . The boundary condition are:

- $v(0,t) = v(L,t) = 0$ ,
- $\partial v / \partial x = 0$  at  $x$  equal 0 and  $L$  for every time step.

The initial ( $t = 0$ ) pressure  $p$ , and density distribution is uniform along the tube and corresponds to atmospheric conditions. Calculations has been carried out for spatial resolution  $\partial x = 1 \text{ m}$  and time step  $\partial t = 0.1 \text{ ms}$ . Mass has been injected in the middle of the tube.

The term  $W$  can be calculated from estimated mass flow rate  $\dot{m}$  which was 20 kg/s. and is expressed in flow mass unit per volume unit i.e.  $\text{kg m}^{-3} \text{ s}^{-1}$ . Allowing for spatial resolution the term can be calculated from equation (10).

$$W = \frac{\dot{m}}{\Delta V} = \frac{\dot{m}}{A_o \Delta x}. \quad (10)$$

This gives the value for  $W$  to be  $2.02 \text{ kg m}^{-3} \text{ s}^{-1}$ . The only trouble is that the assumption that the space volume  $\Delta V$  in which mass production takes place is equal to tube slice of thickness  $\Delta x$  is arbitrary and is assumed only because of chosen spatial distribution. It might as well be higher if one deems that helium is injected in narrower tunnel slice for instance 0.1 m or even less. In conclusion, the internal mass rate production density is uncertain element in this analysis.

Because of the uncertainty the modeling has been carried out for two  $W$  values, one resulting from equation 10 and the second ten times higher, which corresponds to tube slice of thickness of 0.1 m. This is the reason by which of modeling has rather demonstrative character. The Figures 24 and 25 show pressure history for two mass rates in two points of the tube. One in the middle ( $x = 1650$  m) where mass has been injected and the second at the position of  $x = 800$  m.

In case of  $W = 2.02 \text{ kg m}^{-3} \text{ s}^{-1}$  only small pressure variation can be observed in both points which are of the same magnitude i.e. 0.1 bar of overpressure. In case of higher injection rate  $W = 20.2 \text{ kg m}^{-3} \text{ s}^{-1}$  also pressure variation can be observed in both point but now pressure rise at steady rate and no pressure shock is present. Observed high frequency oscillations are result of numerical instability and can be neglected because of small amplitude. Low frequency oscillations seems to be result of tube acoustic and arise from small pressure wave travelling along the tube by turns in both directions because of its reflection from closed ends. In both cases pressure variation in both points seems to be equal in time, save the differences resulting from pressure oscillation, which leads to conclusion that pressure is uniform along the tube with reasonable accuracy during the whole time.

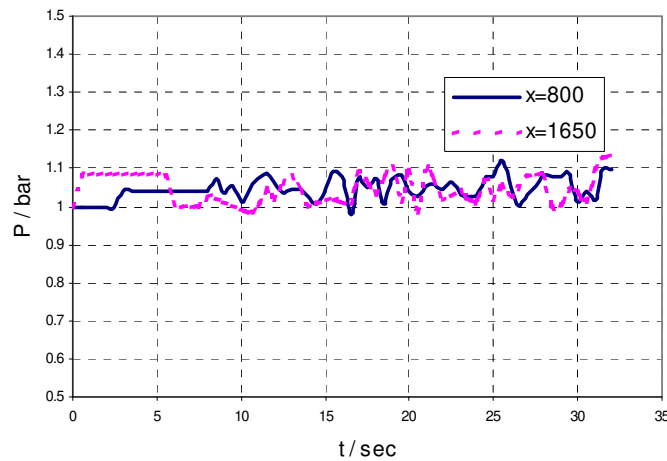


Figure. 24. Pressure history in two points of the tube for mass rate production density equal  $2.02 \text{ kg m}^{-3} \text{ s}^{-1}$  and injection time 60 second.

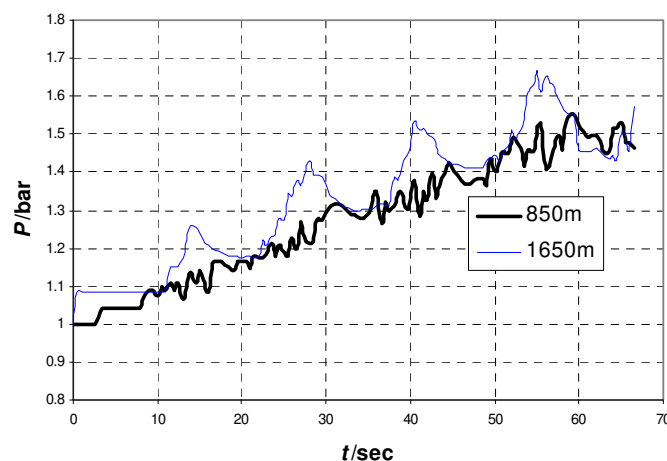


Figure 25. Pressure history in two points of the tube for mass rate production density equal  $20.2 \text{ kg m}^{-3} \text{ s}^{-1}$  and injection time 60 second.

The maximum pressure resulting from helium leakage at the estimated rate of 20 kg/s can be calculated on the basis of static approach. This can be concluded from comparison of possible flow velocity 12.6 m/s what is considerably smaller than sound velocity in air

330 m/s. Also comparison of the time scales is in favour for the above conclusion. The helium leakage time was measured in minutes while pressure wave needs only 10 s to travel along the tunnel section (5 s if injected in the middle). This excludes any shock phenomena and proves that the pressure distribution along the tunnel was practically uniform in time during whole process. Also the numerical modeling underpins the above conclusion. It is easy to see from Figure 25 that no shock phenomenon takes place during wide span of time and pressure growth is steady according to the amount of injected mass.

The Table 6 presents possible pressures that can be attained during incident. The ventilation doors hinges has been estimated to withstand the absolute pressure of 0.113 MPa. This pressure is lower than the pressure listed in Table 6 for leakage of about 1 t of helium at the temperature range 200–300 K (assuming adiabatic air compression). According to calculations the doors should withstand maximum overpressure of magnitude 0.06–0.18 MPa (0.6–1.8 bar). Though for the calculation the worst case has been assumed and real pressures can be smaller, then for safety reason the doors should be designed to withstand the calculated pressure.

## 8. Conclusions

- Preliminary risk analysis of the LHC cryogenic system has been updated, taking into account the experience resulting from the 19th September 2008 incident.
- A new Maximum Credible Incident has been formulated.
- Mathematical modeling based on a thermodynamic approach has shown that the implemented safety relief system protecting the vacuum vessels against over pressurization is characterized by a reasonable safety margin.
- Temporary SV configuration is justified for low energy runs, especially in standard subsectors.
- The tunnel pressurization resulting from significant helium discharge is a static process and no blasting effect can be expected.
- To avoid the tunnel pressurization, self-opening doors or dedicated safety devices should be installed.

## Acknowledgements

This document is the report resulting from the Agreement No. K1619, Addendum 1 - Upgrade on risk analysis following the 080919 incident in the LHC sector 3-4. The authors would like to thank Philippe Lebrun and Antonio Perin for remarks and discussions.

## References

- [1] M. Bajko, F. Bertinelli, N. Catalan Lasheras, S. Claudet, P. Cruikshank, K. Dahlerup-Petersen, R. Denz, P. Fessia, C. Garion, J.M. Jimenez, G. Kirby, M. Koratzinos, Ph. Lebrun (chair), S. Le Naour, K.H. Mess, M. Modena, V. Montabonnet, R. Nunes, V. Parma, A. Perin, G. de Rijk (scientific secretary), A. Rijllart, L. Rossi, R. Schmidt, A. Siemko, P. Strubin, L. Tavian, H. Thiesen, J.Ph. Tock, E. Todesco, R. Veness, A. Verweij, L. Walckiers, R. van Weelderen, R. Wolf, S. Feher, R. Flora, P. Limon, J. Strait, Report of the task force on the incident of 19 September 2008 at the LHC, LHC Project Report 1168, Geneva, 31/03/2009

- [2] M. Chorowski, Ph. Lebrun, G. Riddone, Preliminary risk analysis of the LHC cryogenic system, LHC Project Note 177, 1999-01-12
- [3] M. Chorowski, G. Konopka-Cupiał, G. Riddone, Safety oriented analysis of cold helium - air mixture formation and stratification, *Cryogenics* 2006 vol. **46**, No. 4.
- [4] M. Chorowski, J. Fydrych, G. Riddone, Flow and thermo-mechanical analysis of the LHC sector helium relief system, Proceedings of the Twentieth International Cryogenic Engineering Conference. (ICEC 20), Beijing, China, 11-14 May 2004 / Ed. by L. Zhang, L. Lin, G. Chen. Amsterdam [i in.] : Elsevier, 2005.
- [5] M. Chorowski, Ph. Lebrun, L. Serio, R. van Weelderen - Thermohydraulics of quenches and helium recovery in the LHC prototype magnet strings, *Cryogenics* **38** (1998), 533 – 543.
- [6] Amrogowicz J, Kordylewski W, Wach J, *Gazodynamika przejścia od deflagracji do detonacji w przewodzie* (Gas dynamics of deflagration to detonation transition in tube). Wrocław University of Technology; Raport serii sprawozdania 64/87; Wrocław 1987